A METHODOLOGY TO OBTAIN THE BEST CHARACTERISTIC PARAMETERS OF A BONE REMODELING MODEL WHEN COMPARED TO A CT SCAN BONE DENSITIES DISTRIBUTION

Gabriela Wessling Oening Dicati

José Eduardo Gubaua

Bárbara Belisa Soffiatti

Jucélio Tomás Pereira

gabyoening@hotmail.com

jose.gubaua@yahoo.com.br

bah.soffiatti@gmail.com

prof_jucelio_tomas@hotmail.com

Affiliation

Programa de Pós-Graduação em Engenharia Mecânica - Universidade Federal do Paraná.

Av. Cel. Francisco H. dos Santos, 210, Jardim das Américas, 81.531-970, Paraná, Curitiba, Brasil.

Abstract. *The bone tissue has the capacity of adaptation and renewal and this process is called bone remodeling. Many mathematical models were developed with the purpose of describing this process. These models make it possible to simulate different tissue characteristics, such as bone morphology, anisotropy and visualization of different porosity levels. As a result of these models, we have a distribution of densities that is totally dependent of the parameters used and generate a qualitatively comparison with an X-ray. The major question is that the distribution of femur densities is unique to each individual and, because of empirically determined parameters (such as the width and central position of the dead zone) the model does not quantitatively characterize this individuality. Thus, the objective of this study is to determine the best parameters of the Stanford remodeling model with isotopic behavior, modifying the width and central position of the dead zone, to obtain a distribution of densities that is as similar as possible to a computational tomography. For the development of this study, concepts of metamodel and optimization are employed. Numerical simulations of bone remodeling are performed using the Finite Element Method through the software Abaqus.*

Keywords: *Bone Remodeling, Finite Element Method, Characteristic Parameters, Metamodeling, Computed tomography.*

Proceedings of the XXXVIII Iberian Latin-American Congress on Computational Methods in Engineering P.O. Faria, R.H. Lopez, L.F.F. Miguel, W.J.S. Gomes, M. Noronha (Editores), ABMEC, Florianópolis, SC, Brazil, November 5-8, 2017.

1 INTRODUCTION

The bone is a living tissue that has extreme complexity due to its structure present porous regions, high heterogeneity and anisotropy (García et al., 2002). Another characteristic of the tissue is that it is under constant change of its structure due to internal and external signs for example, hormonal influences, external mechanical loads and among others. This process of structural adaptation is called bone remodeling (Doblaré; García, 2001; Lemaire et al., 2004). This process occurs throughout life and is characterized by the replacement of the old and damaged tissue by a new and healthy one (Lemaire et al, 2004).

Due to bone is a living tissue, it has the ability to restore itself through bone remodeling as well as becoming sick. In the case of the human femur, diseases such as osteoarthritis, which affects cartilage and, subsequently, bone tissue, femoral head osteonecrosis and rheumatoid arthritis are examples of abnormalities that impair the life quality of the human being. One of the ways of treating these diseases is the insertion of a prosthesis in the femur, this changes the distribution of loads along the bone, which induces an adaptation of the tissue. With the placement of the prosthesis, the loads are applied directly to the component that transmits the loads to the bone. Thus, this transmission can lead to a level of accentuated loss of bone density (stress shielding) or even, a fracture. Adaptation occurs in a unique way for each individual, even though the same type of component is inserted (Fig. 1). This occurs because of unique characteristics regarding loading, adaptation, sex, age, level of daily physical exercises, feeding, hormonal activity among others.

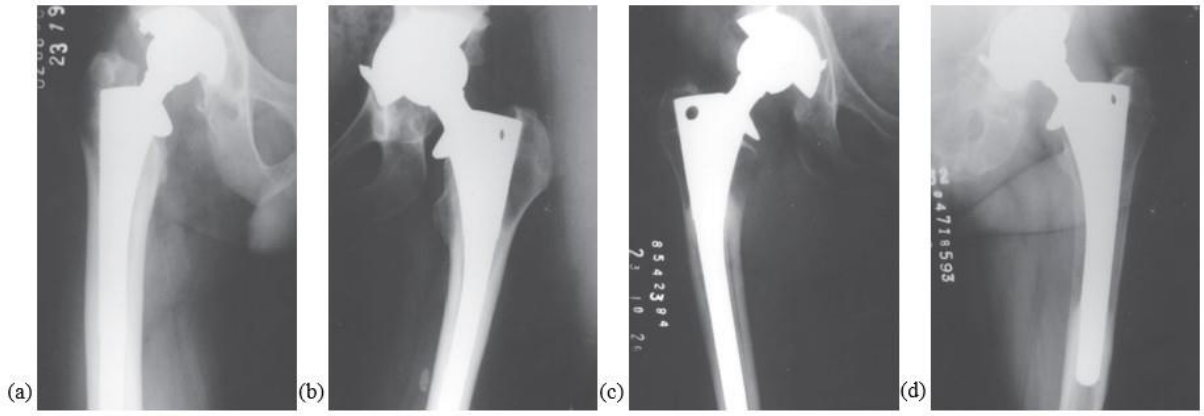

Figure 1. Femoral bone adaptation of four patients after THA surgery with the same kind of prosthesis. (a) Densities distribution without stress shielding, (b) with low-level, (c) moderate-level and (d) high-level of stress shielding. (Alencar, 2007).

It is possible to simulate the behavior of the tissue according to the application of loads. In the case of the femur, when loads acting on a walk are applied, for example, it is possible to obtain a distribution of densities. This characterizes the morphology of the femur in a qualitative way in its stable distribution. Figures 2(a) and 2(b) present a human femur x-ray and a numerical density field, obtained from a mathematical model of bone remodeling, respectively. It is noted that there are discrepancies between the numerical and real densities distributions, where the first one is just a qualitative representation, as previously stated. The distribution of numeric densities that is as close as possible to the actual distribution is difficult to obtain, due to the fact that each person has a singular field (Fig. 3). In addition, the parameters of the bone

Proceedings of the XXXVIII Iberian Latin-American Congress on Computational Methods in Engineering P.O. Faria, R.H. Lopez, L.F.F. Miguel, W.J.S. Gomes, M. Noronha (Editores), ABMEC, Florianópolis, SC, Brazil, November 5-8, 2017.

remodeling models are generally determined empirically, without an ideal or optimal configuration for every person.

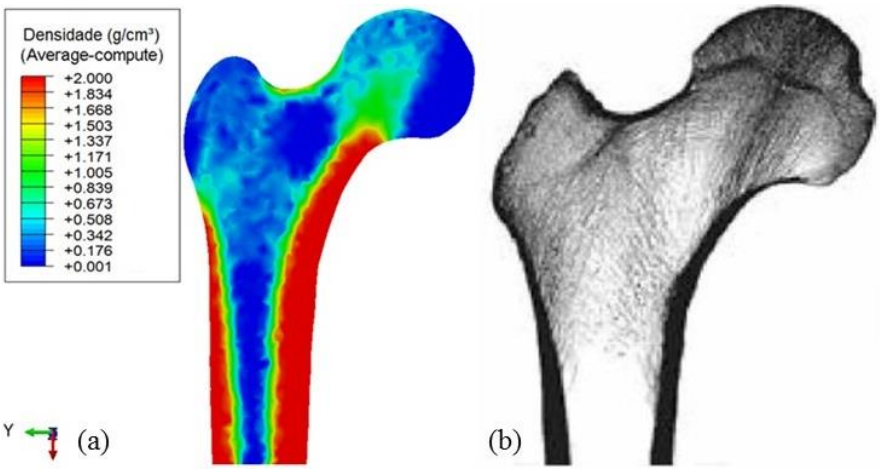

Figure 2. (a) Numerical and (b) clinical bone densities field. (Dicati, 2015; Jacobs, 1994).

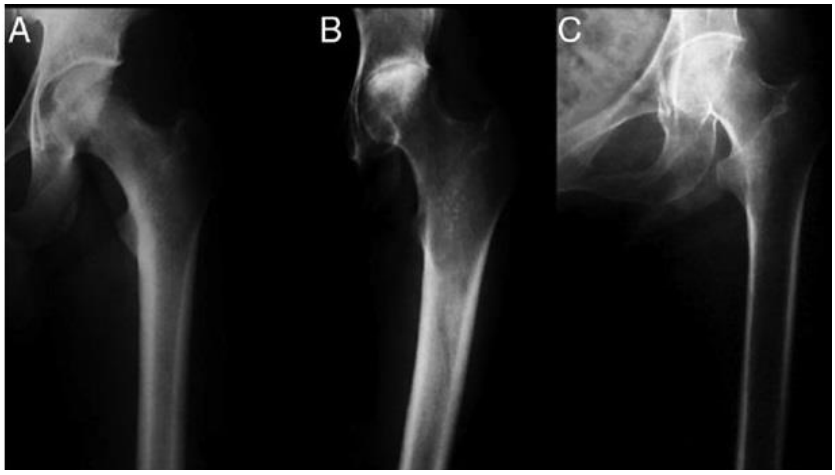

Figure 3. Radiographies of different morphologies (A, B, C) found in femur. (Hatem et al., 1994).

It is evident from Fig. 2 and 3 that there are differences between the distributions, whether clinical in relation to the numerical or even between the clinics ones. This difference is influenced by a visual character and numerical variation. This variation is minimized, in direction to obtaining the best parameters for a given model of bone remodeling. Thus, the numerical distribution can represent the real one in an appropriate way. Finally, this model is applied uniquely and exclusively to the individual who has that distribution.

The verification of a bone remodeling model which recreates the density distribution corresponding to the applied load is an initial and essential step that must be performed, for example, previously to the installation of a prosthesis and requires a refinement of the model parameters.

Following this concept, Thomsen et al. (1996) made a sensitivity analysis on the parameters of the remodeling model, in order to obtain a density configuration of a vertebra that is similar to that found after the menopausal period. The model describes the effects of two parameters on the loss of vertebral trabecular tissue. The simulation is made over a period of 20 years, where initially considers that the bone is of a 48-years person, and that the end of menopause

occurs 5 years after the simulation starts. The sensitivity analysis is made for two parameters of the model, which are the activation frequency that has its value doubled (de 1/1096 days^{-1} for 1/548 days^{-1}), and the depth of resorption that is increased from 50 to 70μm. After menopause (5 years), it is assumed that these parameters return to their initial values.

The bone remodeling model proposed by Huiskes et al. (1992) is modified by Turner et al. (2005). In this study, this model is combined with a three-dimensional geometric model of a human femur discretized by FEM to predict changes in bone density after THA. The simulation is made for three femoral components with different designs (component geometry and applied material). The following parameters are modified in the model of bone remodeling: (a) formation and resorption bone rate, (b) center position of dead zone, (c) loading application and (d) mechanical stimulus. The Gruen zones densities are qualitatively related to the measurements of clinical densitometry (DEXA) after a period of two years of the THA installation.

According to Tsubota e Adachi (2005), the parameters of the remodeling model are the keys to the determination of spatial and temporal changes in bone structure, in a computational simulation. In this sense, the authors vary different parameters in order to describe the changes in the trabecular structure. Two parameters are introduced in the equation of the remodeling rate to express the sensitivity of bone cells in relation to the mechanical stimulus, which are the limit values of the dead zone and sensing distance (Defined as the radius of the area where cells can "feel" the mechanical stimulus). The authors adopt the sensing distance as constant and they vary the limits of the dead zone (from 0 to 10) for some analysis. In a second approach, the authors vary the sensing distance, normalizing it by the length of the trabecular bone in the region, and stimulating a constant dead zone, with interval of ±5,0.

Sharma et al. (2009) aim in their study to complete the first step towards the development of a realistic model, robust and subject to a specific loading, that makes it possible to simulate the process of bone remodeling of a glenoid. In this study the bone remodeling of the glenoid is a process given by the strain energy. This is determined by applying the bone remodeling model proposed by Weinans et al. (1992). The authors vary some parameters of the remodeling model randomly. According to the authors, the best configuration is where it is obtained a distribution that allows the visual comparison with clinical one and that is very similar qualitatively of the real distribution.

The capacity of the bone remodeling model proposed by Doblaré e García (2002) to predict the distribution of densities of different types of human bones (femur, tibia and mandible) is evaluated by Pérez et al. (2010). The model is used with the parameters suggested by Doblaré e García (2002). To evaluate the model capacity they made a quantitative comparison between the density distributions calculated by Computerized Tomography (CT) data and the one simulated by the bone remodeling model. A code is implemented, via Matlab, to calculate the absolute and relative errors and made the comparison between the distributions. The absolute error is obtained by means of the difference between the density fields relative to the remodeling model and calculated from the HU, obtained from the CT. The relative error is calculated dividing the absolute error by the density obtained in the CT. The smallest errors are found in the cortical regions, where the density is higher. With the decrease of the density value, an increase in error was obtained. The largest errors are found in the regions where boundary conditions were applied.

Likewise, Sharma et al. (2009) work, where one model of femoral bone remodeling is applied to another bone, Neuert e Dunning (2013) apply the Weinans et al. (1992) model for the simulation of the distal epiphyses of the ulna. In this work, the authors vary the parameters of reference stimulus (randomly adopted) and dead zone (with values found in the literature). For evaluation, an error measure, called the mean square error, is applied. This evaluates the difference between the clinical and numerical fields of densities within a region of interest.

This study aims to propose, implement and test a methodology to characterize the parameters of bone remodeling models to obtain a numerical densities field similar to the field of a given computed tomography of the human femur. In this study will be used the parameters of reference stimulus and dead zone of the model of bone remodeling proposed by Jacobs (1994). The solid model is reconstructed using a computerized tomography and FEM is discretized using quadratic tetrahedral elements on Abaqus software.

2 MATERIALS AND METHODS

In this chapter we present the methodology used in this study, as well as the bone remodeling model, the femur geometry and the finite element model with respective boundary conditions.

2.1 Methodology

The methodology applied to the development of this study is divided into three stages. The first stage refers to the construction of the solid femur model and the assignment of the densities of a specific CT. The second one refers to the simulations of the bone remodeling process of the finite element model obtained from the previous solid. Finally, the applications of the experimental design, metamodeling and optimization techniques to construct a methodology that allows to obtain the optimal parameters of the remodeling model for the provided CT.

2.1.1 Construction of the solid model and attribution of densities

Figure 4 shows a flowchart with the steps necessary for constructing a solid model of a human femur from a CT. Invesalius software allows the isolation of different tissues that compose the human body, through the Hounsfield scale. Obtaining the contour of the human femur depends exclusively on the Hounsfield values representing the bone tissue. Subsequently, MeshMixer software is used for surface treatment generated by Invesalius. This software allows the removal of unwanted surfaces, remesh, smoothing of the surface and filling of holes. Finally, SolidWorks allows the transformation of the femur surface into a solid model.

After the construction of the solid model, it is made the definition of real densities. Here two softwares are used. The first one, Abaqus, generates a finite element mesh and text files with information relative to the nodal coordinates connectivity of the elements. The second one is the BoneMat, which assigns the densities of the tomography to the elements of FEM model. To assign the densities to the mesh, these information together with DICOM files are used as input data in BoneMat.

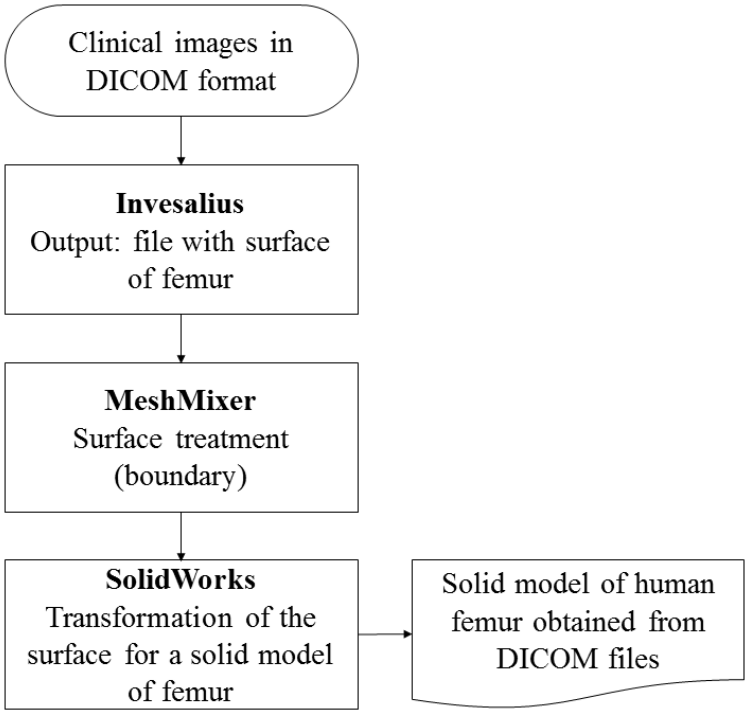

Figura 4. Flowchart for building a solid bone model.

2.1.2 Computational bone remodeling

The second step of this study, presented in the flowchart of Fig. 5, consists in obtaining a field of numerical densities, which allows the comparison with the distribution of a real femur. For this, a FEM analysis is made on Abaqus coupled with subroutines developed in Fortran language. The isotropic Stanford bone remodeling model is used in this study and presented later.

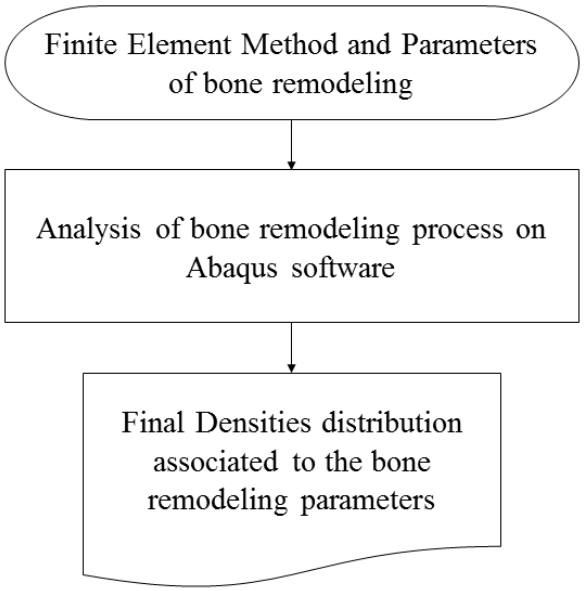

Figure 5. Generic flowchart of bone remodeling process.

2.1.3 Construction of the general structure

The flowchart shown in Fig. 6 represents the third step of this study and show an overview of the methodology to be implemented. The first step is the definition of the bone remodeling model. Then, it is identified and limited the bone remodeling parameters that may cause variations according to the individual (the width and central position of the dead zone are considered for this study). The next step is the assembly of the structure with the Latin Hypercube method and Kriging metamodeling.

After the definition of parameters and methods, it is generate samples that will compose the design of experiments (DOE). Each sample has a set of parameters $\mathbf{x}^{(i)}$, which is used as input data in the bone remodeling model and generates a numerical densities field, $\rho\left(\mathbf{x}^{(i)}\right)$. The difference between this numerical field and that one obtained on CT, ρ_{CT}, is determined by an "error" function, F_{error}, such as

$$"error" = F_{error} = F\left(\rho\left(\mathbf{x}^{(i)}\right) - \rho_{CT}\right) = \frac{100}{\rho_{cb}}\left\{\frac{1}{NEl}\sum_{j=1}^{NEl}\left[\rho^{j}\left(\mathbf{x}^{(i)}\right) - \rho_{CT}^{j}\right]^{2}\right\}^{1/2}, \tag{1}$$

where NEl is the number of elements of the FEM mesh and ρ_{cb} is the maximum value for cortical bone tissue. The value of this function will compose the DOE. The “error” is determined for each sample of DOE and then it is possible to construct an initial response surface (metamodel).

After defining the initial response surface, an infill criterion is used to improve the constructed function and to determine a new point $\mathbf{x}^{(i)}$, which is expected to have a better value for "error" function, that is, a smaller value than initial samples. In this study we used as infill criterion the probability of improvement and the expected improvement (Forrester, 2008). This point is added to the DOE experiments and generates a new response surface. This process is repeated until the optimal point to be determined.

Thus, the optimal point represents the set of parameters of the bone remodeling model used, which results in the best approximation of the densities distribution obtained in a CT. That is, these parameters represents quantitatively the patient analyzed by the CT.

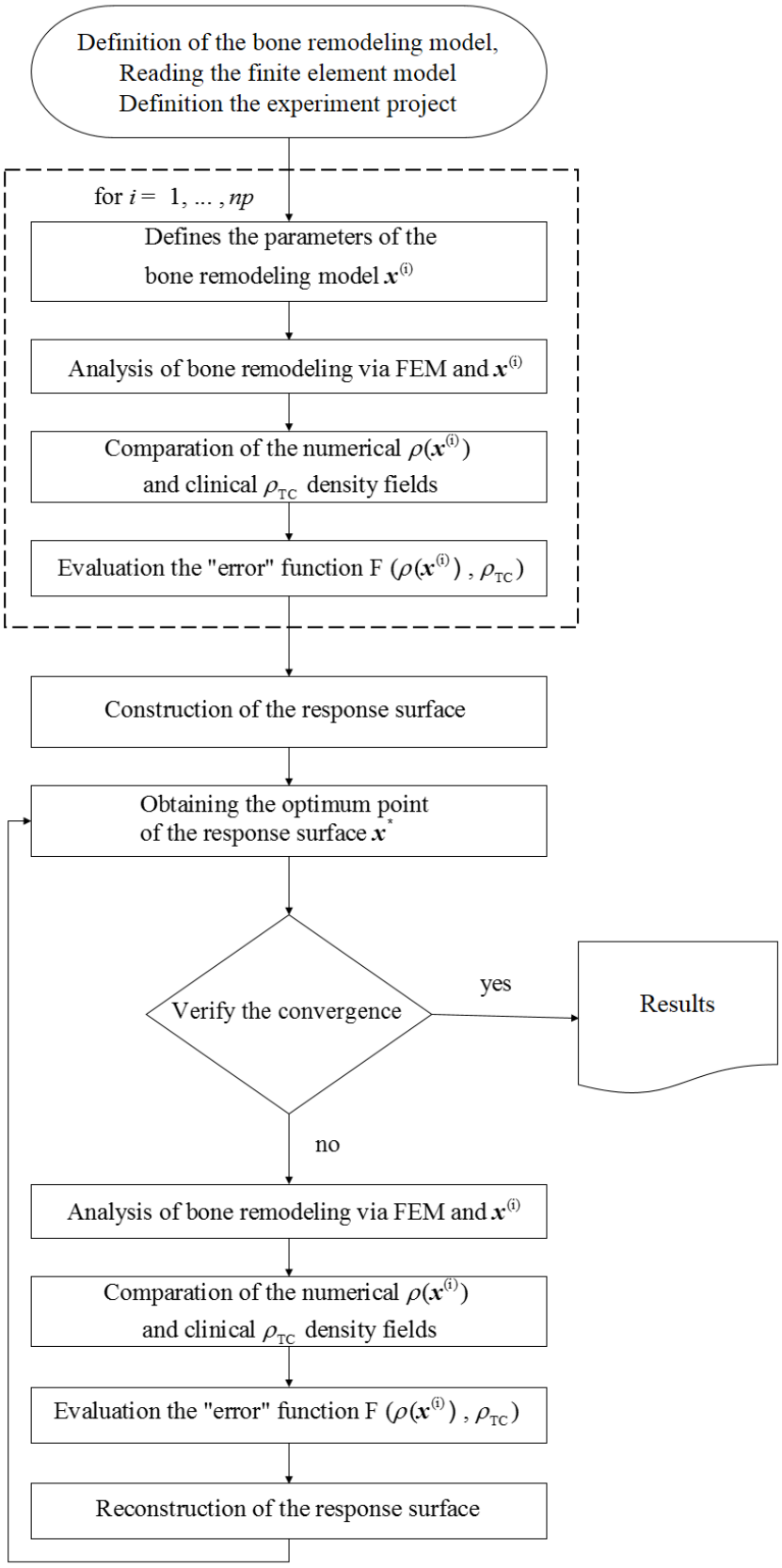

Figure 6. General flowchart used in this study.

2.2 Bone remodeling model

The Stanford isotropic bone remodeling model (Jacobs et al. 1995) is developed based on Beaupré et al. (1990), which defines the bone tissue with elastic, linear and isotropic behavior. The bone remodeling model assumes that bone tissue has the capacity to adapt to a load, after a daily tissue stress stimulus, Ψ_t, which is determined as

$$\psi_t = \left(\sum_{dias} n_i \overline{\sigma}_{t_i}^{m} \right)^{\frac{1}{m}} \tag{2}$$

where n_i is the number relative to the daily load cycle applied to the bone tissue related to the loading of the type i, $\bar{\sigma}_{t_i}$ is the scalar that quantifies the intensity of the effective stress on tissue that is related to the applied load and m is an empirical constant, which quantifies the stress state occurred related to the number of cycles (Corso, 2006).

The daily tissue stress stimulus is the scalar that governs the whole bone remodeling process and acts directly linked to the rate of bone remodeling $\dot{r}$. This rate indicates the possible changes that may occur according to the daily tissue stress stimulus. The behavior of $\dot{r}$ is shown in Fig. 1. It is observed three types of bone tissue response. When the daily tissue stress stimulus is greater than the reference value, bone tissue formation will occurs. For the stimulus smaller than the reference value, there is bone resorption. The central region of Fig. 1 is called dead zone, where there is no changes on properties, that is, that point is a stable state. Thus, the rate of remodeling $\dot{r}$ is defined as

$$\dot{r} = \begin{cases} c\left[\left(\psi_t - \left(\psi_t^* - \psi_z\right)\right)\right] & if \quad \psi_t < \left(\psi_t^* - \psi_z\right), \\ 0 \qquad\qquad if & \left(\psi_t^* - \psi_z\right) < \psi_t < \left(\psi_t^* + \psi_z\right), \\ c\left[\left(\psi_t - \left(\psi_t^* + \psi_z\right)\right)\right] & if \quad \psi_t > \left(\psi_t^* + \psi_z\right). \end{cases} \tag{3}$$

In this case, Ψ_t^* is the reference daily tissue stress stimulus, c is the remodeling speed and Ψ_z is half-width of dead zone.

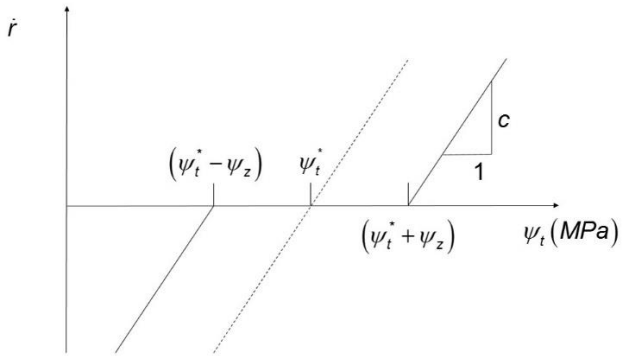

Figure 7. rate of remodeling ($\dot{r}$) behaviour.

The material density updates is dependent on a function that determines the rate of the evolution of densities ($\dot{\rho}$), which is given by

$$\dot{\rho} = k\, S_v\, \dot{r} \rho_c, \tag{4}$$

where k is a parameter that defines the percentage of active surface and S_v is the specific surface area. The last one is a parameter that quantifies the internal tissue surface by volume density. Finally, the update of apparent density for each point of the bone tissue is determined as

$$\rho^{(n+1)} = \rho^{(n)} + \dot{\rho}^{(n)} \Delta t, \tag{5}$$

where $\rho^{(n+1)}$ is the updated density, $\rho^{(n)}$ is the current density e Δt is the time interval relative to the cycle of the remodeling process. Table 1 presents the necessary constants for Stanford isotropic bone remodeling.

Table 1. Constants used in computational analyses of Stanford model (1994)

Parâmeters	Value	Unit
c	2.0×10^{-5}	(mm/day)/(MPa/day)
ψ_t^*	50.0	MPa
m	4.0	-
n_i	3000	Cycles/day
ψ_z	$0.125 \times \psi_t^*$	MPa
ρ_c	2.0	g/cm³
Δt	7	Day
K	1.0	-

2.3 Finite element model

The analysis of bone remodeling process is carried out on a three-dimensional human femur solid model reconstructed using a CT and presented in Fig. 7. The model is simulated on Abaqus software through the UMAT subroutine (User Material) and it is discretized in 114,961 quadratic tetrahedral elements, named C3D10 (Continuum, three-dimensional with 10 nodes), and 164,524 nodes.

The load case is presented by Gubaua (2016) e Dicati (2015) and it is seen in Fig.8. This load case was developed using the intensities presented by Beaupré et al. (1990); the areas of load application on femoral head presented by Greenwald e Haynes (1972); and the directions and areas of application on greater trochanter presented by Bagge (1999). The load case is composed by six loads which characterize one step of a gait. These loads are derivate by two mean sources. The first one refers to the compression forces on femoral head, which occur due

to the contact with the acetabulum. The second source refers to the reaction of muscular forces (traction loading) on greater trochanter. Table 2 shows the intensities and orientation of the applied forces on femur.

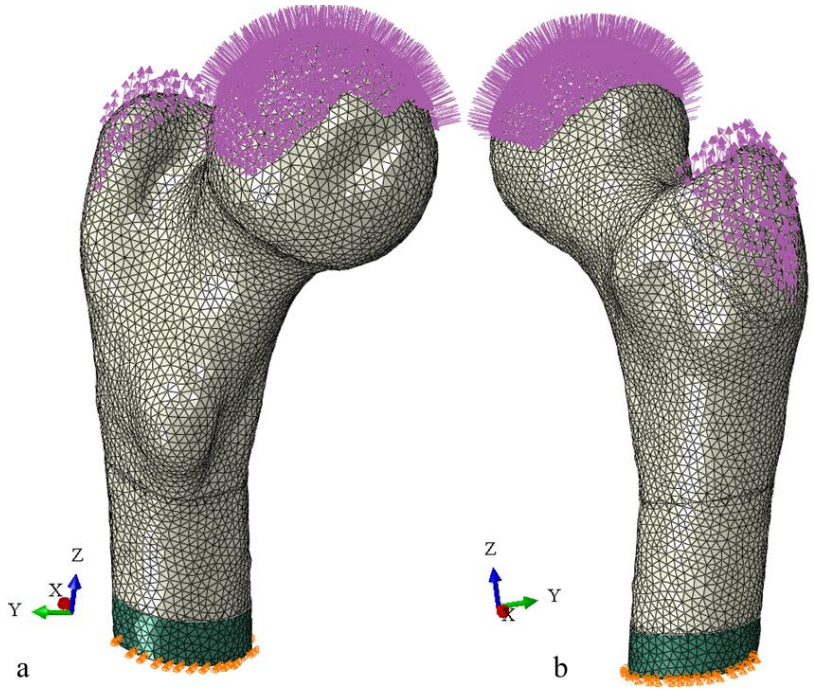

Figure 8. Load case (Gubaua, 2016; Dicati, 2015).

Table 2. Intensity and orientation of load applied on proximal human femur in 3D analysis.

Load	Intensity (N)	Orientation (grades)[1]
Compression – 1	1158	Pressure (normal to surface)
Compression – 2	2317	Pressure (normal to surface)
Compression – 3	1548	Pressure (normal to surface)
Traction – 1	351	27,53; 29,3; 59.65
Traction – 2	703	-5,933; 2,848; 39,29
Traction – 3	468	23,28; -27,93; 62,17

[1]Coordinate system is orientated with x-axis in lateral-medial direction, y-axis anterior-posterior direction and z-axis for lower-upper direction.

Homogeneous Dirichlet boundary conditions are applied on a solid with elastic, isotropic and linear solid behavior fixed on femoral diaphysis. This is made to avoid stress concentrations. All analysis start with a homogeneous configuration of densities of $1.0e^{-6}$ kg/mm³.

3 RESULTS AND DISCUSSIONS

Two simulations of Kriging response surface were performed to obtain the results of this study. The first one is shown in Fig. 8. The initial response surface was constructed with 30 sample (black dots) determined using Latin Hypercube and 14 samples (green dots) were added on analyses following the expected improvement and probability of improvement criteria.

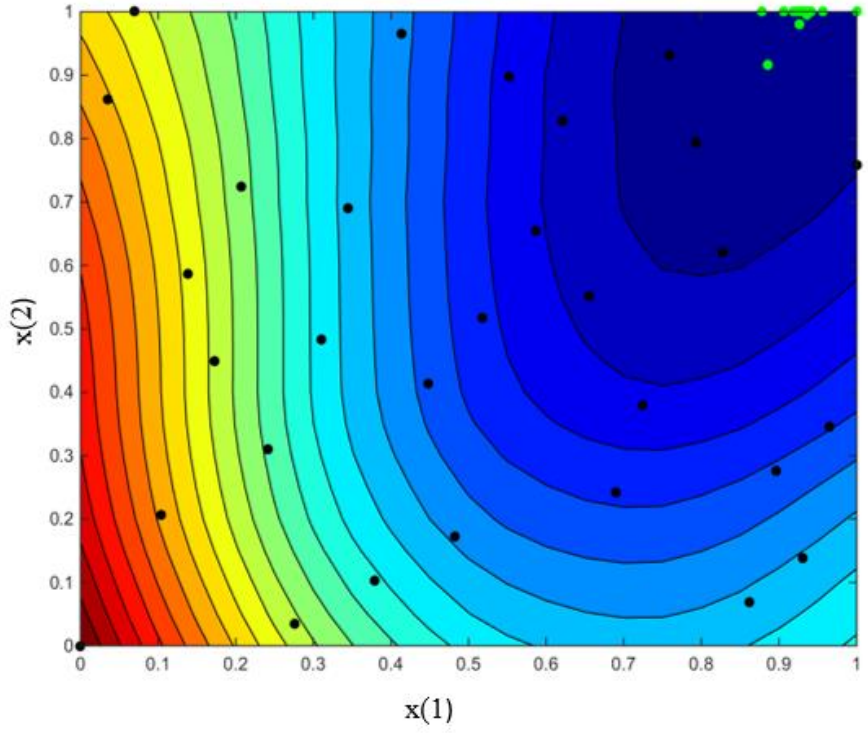

Figura 9. Initial response surface (black dots) and samples added (green dots).

For the first analysis we adopted that the variation of the center and half-width of dead zone is defined respectively by the equations

$$\psi_t^* = 40 + 60\mathbf{x}(1) \tag{6}$$

and

$$\psi_z = 20\mathbf{x}(2), \tag{7}$$

where **x**(1) and **x**(2) are the parameters of DOE that vary between 0 and 1. Therefore, x(1) (reference value for daily tissue stress stimulus) has a maximum and minimum value of 100.0 MPa and 40.0 MPa respectively. The second parameter **x**(2) (half-width of dead zone) has the maximum and minimum values of 20.0 MPa and 0.0 MPa respectively. This region has the reference parameters values (Jacobs et al., 1995) presented in Table 1.

For this analysis, the best set of parameters, that is, the lowest value of the F_{error} is found in the coordinates **x**(1) equal to 0.937703 and **x**(2) equal to 1.000. That is, the daily tissue stress stimulus ψ_t^* is 96.26218 MPa and the half-width of dead zone ψ_z is 20.00 MPa. For this set of parameters, the function error F_{error} is 21.3615%. The reference parameters (Jacobs et al.

1995) generate a densities distribution that has F_{error} equal to 29.2344 % in relation to the densities distribution obtained from CT.

As seen in Fig. 9, the lowest value of the F_{error} coincided with the boundary imposed by the equations. Thus, a new analysis was performed in order to increase the viable region of the analysis and to verify the response surface behavior.

In first response surface, the minimum values for F_{error} were found in a region that started around the coordinates of 0.7 for both **x**(1) and **x**(2). Thus, the second response surface has samples with coordinates that has theses values as reference. The equations that mapping the region and quantify the variation of the width and center of the dead zone were modified for the second analysis in order to increase viable region, given by

$$\psi_t^* = 70 + 80\mathbf{x}(1) \tag{8}$$

and

$$\psi_z = 10 + 30\mathbf{x}(2). \tag{9}$$

In these equations, **x**(1) and **x**(2) keep varying between 0 and 1. Therefore, x(1) (reference value for daily tissue stress stimulus) has a maximum and minimum value of 70,0 MPa and 150,0 MPa, respectively. The second parameter **x**(2) (half-width of dead zone) has the maximum and minimum values of 10.0 MPa and 40.0 MPa, respectively.

The result of this second analysis is presented in Fig. 10. In this analysis, the surface response is composed by 64 dots, whether black (initial sample) or green, where those could be added from the previous analysis or from the expected improvement and probability of improvement criteria. After the two analysis, it was verified that the lowest value of the "error" function is found in the second analysis and is given by the coordinates **x**(1) equal to 0.473304 and **x**(2) equal to 0.715436, that is, the reference daily tissue stress stimulus ψ_t^* has a value of 107.86432 MPa (2,157 times greater than the reference value (Table 1)) and the half-width of dead zone ψ_z is 31.46308 MPa (2,517 times greater than the reference value (Table 1)). These coordinates generate a densities distribution with F_{error} equal to 21.1801%, which improves minimally the results obtained in first analysis.

Figure 11 shows bone densities distribution obtained from CT scan (Fig. 11a), for the lowest value for F_{error} found in second analysis (Fig. 11b) and for reference parameters (Fig. 11c) presented by Jacobs et al. (1995). For the last two numerical distributions (Fig. 11b and 11c), we note the mean morphological characteristics found in a human femur (Fig. 11a), as cortical and medullary cavity formation around and inside the femoral diaphysis, respectively; trabecular densities on greater trochanter and femoral head regions.

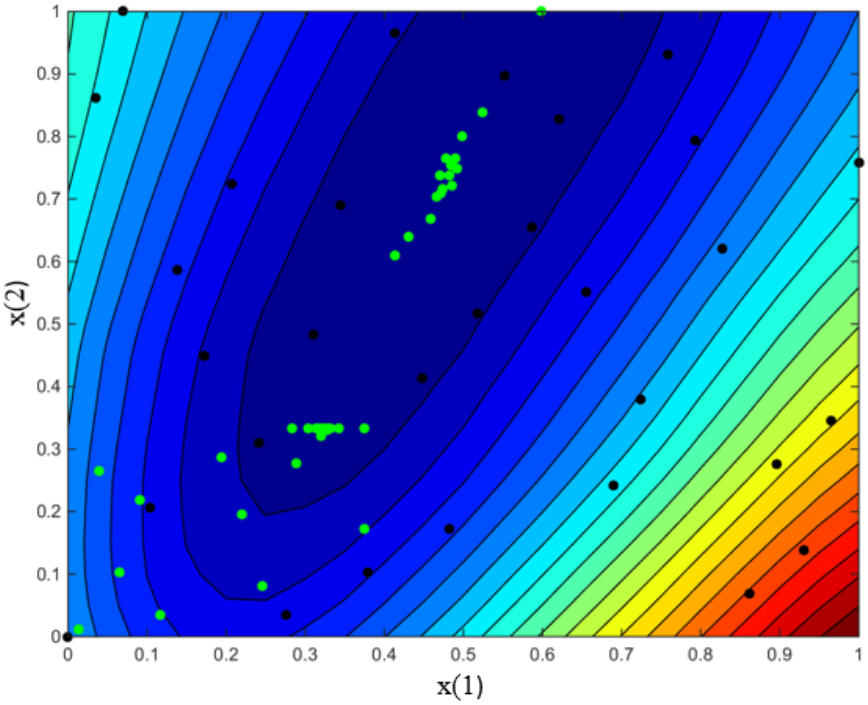

Figure 10. Second response surface used in this study.

Bone densities distribution obtained for reference parameters (Fig. 11c) provides discrepancies when compared with CT scan densities distribution (Fig. 11a). That distribution presents thick cortical, a narrow medullary cavity and a proximal epiphyses with high-density values. Other important point is that the reference parameters characterize the bone densities distribution just in a qualitative way. The discrepancies decrease when CT scan densities distribution is compared with densities field for the lowest value for F_{error}.

Figure 12 shows the elementary "error" ($error_{el}$), which is the comparison between best sample of the second analysis and CT scan densities fields and determined as

$$error_{el} = \frac{100}{\rho_{cb}} \left\{ abs\left[\rho^j\left(\mathbf{x}^{(i)}\right) - \rho^j_{CT} \right] \right\}. \tag{10}$$

We note in Fig. 12 the biggest values for $error_{el}$ are found in regions where there is transition between cortical and trabecular bone tissues. Other region that has a high influence on $error_{el}$ values is the lesser trochanter. On the other hand, we observe that $error_{el}$ is zero or close to it for well-defined regions (cortical bone tissue and medullary cavity on femoral diaphysis).

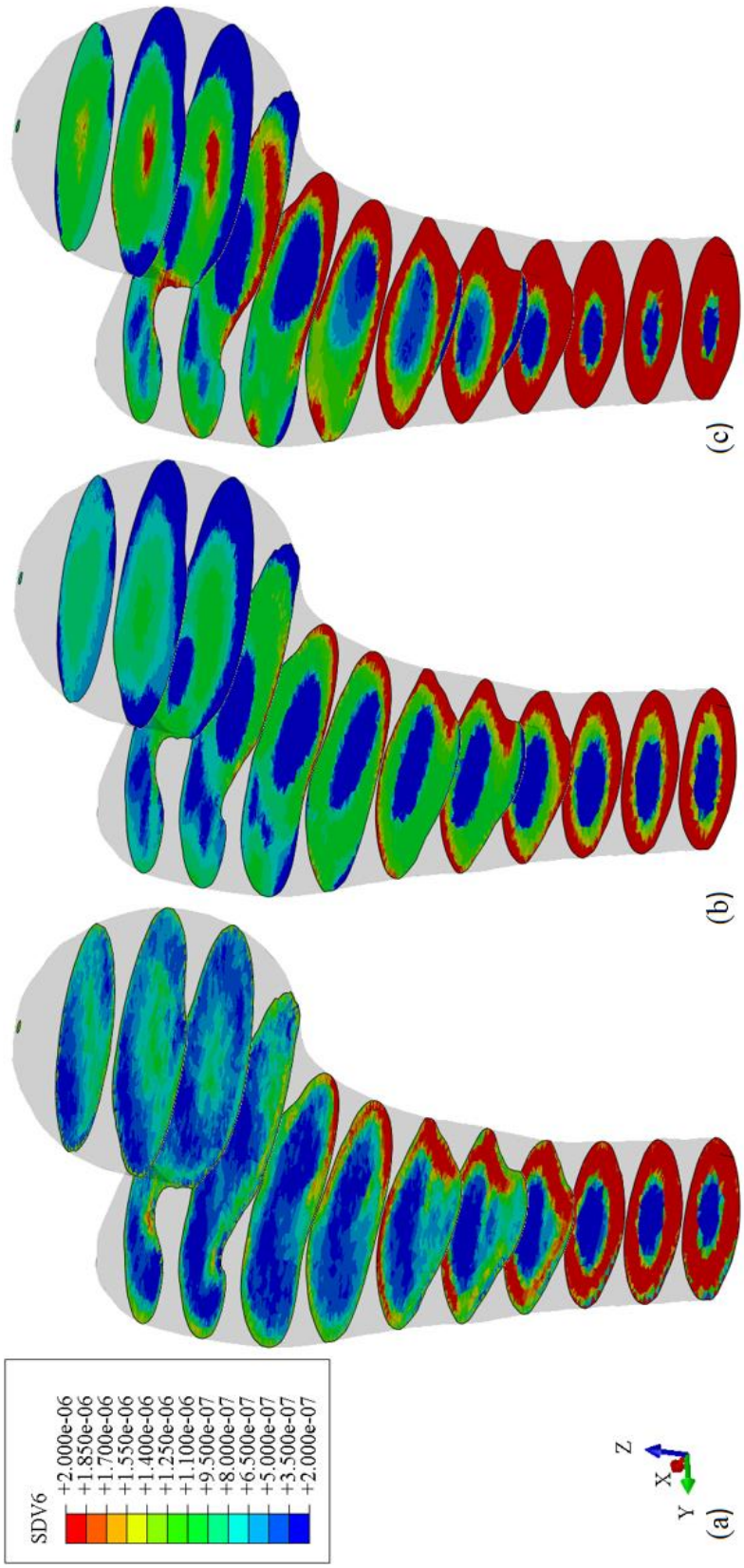

Figure 11. Bone densities distribution obtained (a) from CT scan, (b) for the lowest value for F_{error} found in second analysis and (c) for reference parameters presented by Jacobs et al. (1995) (SDV6 in kg/mm³).

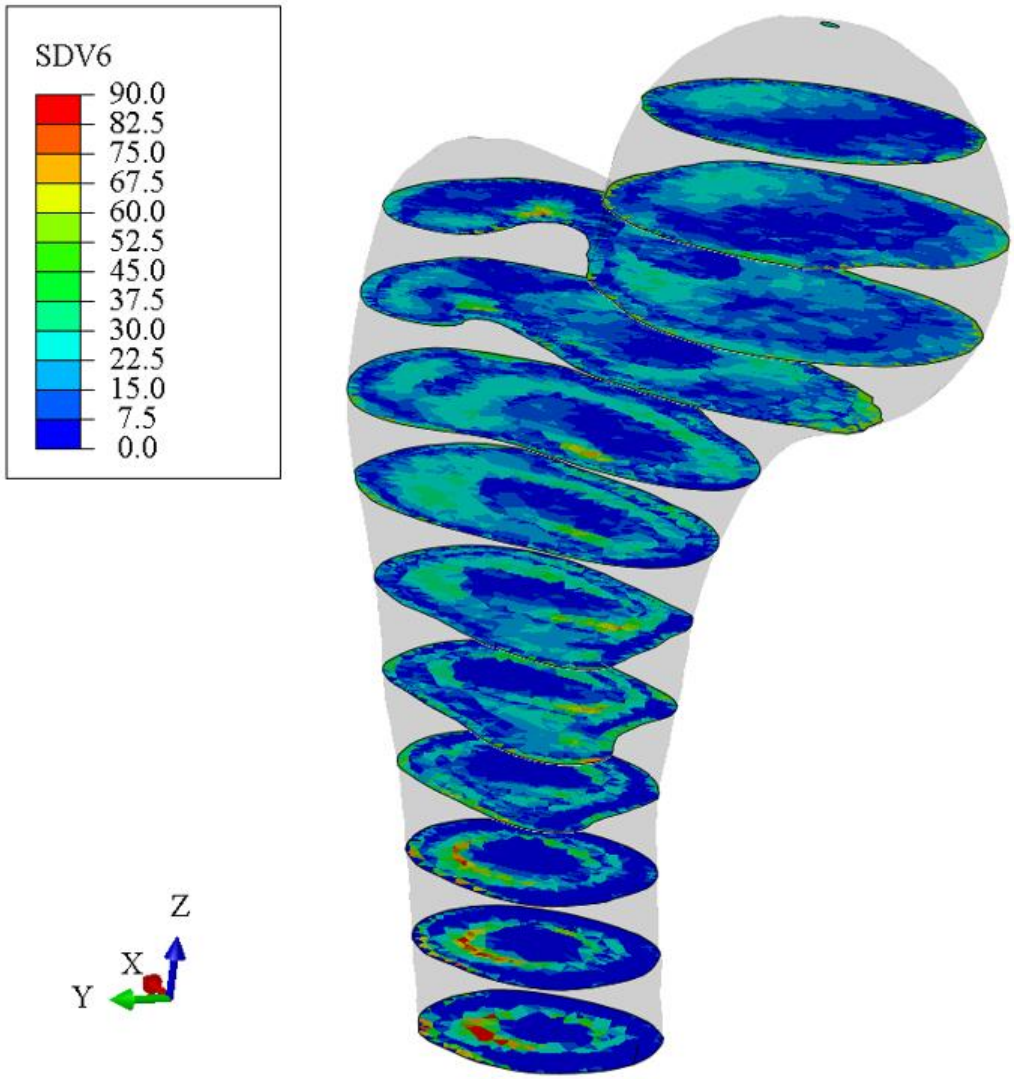

Figure 12. Elementary "error" distribution for the lowest value for F_{error} found in second analysis (SDV6 in %)

4 CONCLUSIONS

This study aims to develop a methodology to obtain the best parameters for a bone remodeling model when compared with a CT scan. The results are preliminary, but they present a meaningful improve of F_{error} in relation with reference parameters. We note that the F_{error} decreases one-third and these results are going in direction to a quantitative comparison with a CT scan. The variation of parameters allows to obtain a densities field that represents effectively the femoral morphology.

There are some point to improve the results. First observation could be done for the number of parameters modified in analysis. Here, just the reference value for daily tissue stress stimulus and the width of dead zone was modified and the bone remodeling model presents other parameters to do that as the empirical constant *m* or percentage of active surface *k.* A second observation is that the bone remodeling model used is simple and isotropic, therefore others complex models also could be analyzed to evaluate the methodology and improve the results. The third point is the reconstruction of CT scan. This is one of the most important steps in methodology and an incorrect bone densities distribution obtained from CT scan could affect drastically the results. Finally, the load case. In human femur there are muscle insertions along the femoral diaphysis, greater and lesser trochanters besides other regions on epiphysis. The load case of this study and several others found in literature apply just the forces on greater trochanter (muscles) and femoral head (contact with acetabulum). Muscles as psoas and illiacus should be considered on lesser trochanter to improve the results.

Although some improves must be necessary yet, this methodology allows to characterize the bone tissue and also to assist the project of prosthesis for that individual.

Proceedings of the XXXVIII Iberian Latin-American Congress on Computational Methods in Engineering P.O. Faria, R.H. Lopez, L.F.F. Miguel, W.J.S. Gomes, M. Noronha (Editores), ABMEC, Florianópolis, SC, Brazil, November 5-8, 2017.

REFERENCES

Bagge, M., 1999. *Remodeling of bone structures.* PhD Thesis, Technical University of Denmark.

Beaupré, G.S., Orr, T., Carter, D. R., 1990. An approach for time-dependent bone modeling and remodeling – Theoretical development. *Journal of Orthopaedic Research*, vol. 8. Pp. 651-661.

Boschin, L. C., Alencar, P. G. C., 2007. Avaliação radiográfica após seguimento a longo prazo. *Revista Brasileira de Ortopedia*, v. 42, pp. 290 – 296.

Corso, L. L., 2006. *Aplicação de procedimentos de otimização e remodelamento ósseo na simulação e análise de problemas de biomecânica*. Master Thesis, Federal University of Rio Grande do Sul.

Dicati, G. W. O., 2015. *Análise comparativa entre os modelos de Stanford isotrópico e anisotrópico para remodelação óssea utilizando o método dos elementos finitos 2d e 3d.* Master Thesis, Federal University of Paraná.

Doblaré, M., García, J. M., 2001. Application of an anisotropic bone-remodelling model based on a damage-repair theory to the analysis of the proximal femur before and after total hip replacement. *Journal of Biomechanics*, vol. 34, pp. 1157-1170.

Doblaré, M., García, J. M., 2002. Anisotropic bone remodelling model based on a continuum damage-repair theory. *Journal of Biomechanics*, v. 35, n. 1, pp. 1 – 17.

Forrester, A. I. J., Sóbester, A., Keane, A. J., 2008. *Engineering design via surrogate modelling: A practical guide*. 1. ed. Pondicherry, India: John Wiley & Sons.

García, J. M., Doblaré, M., Cegoñino, J., 2002. Bone remodelling simulation: A tool for implant design. *Computational Materials Science*, v. 25, n. 1–2, pp. 100 – 114.

Greenwald, A.S., Haynes, D.W., 1972. Weight-bearing areas in the human hip joint. *The Journal of Bone and Joint Surgery*, vol. 54, pp. 157-163.

Gubaua, J. E., 2016. *Análise numérica da influência da rigidez de próteses femorais no processo de remodelação óssea associado à técnica cirúrgica de Artroplastia total de quadril.* Master Thesis, Federal University of Paraná.

Hatem, M. A., Luz, B. F. da, Nishi, R. N., Alencar, P. G. C. de., 2014. Avaliação dos resultados de componente femoral cônico de fixação proximal não cimentado em fêmur tipo C de Dorr. *Revista Brasileira de Ortopedia*, v. 49, n. 3, pp. 260 – 266.

Huiskes, R., Weinans, H., Rietbergen, B. van, 1992. The relationship between stress shielding and bone resorption around total hip stems and the effects of flexible materials. *Clinical Orthopaedics and Related Research*, n. 274, pp. 124–134.

Jacobs, C. R., 1994. *Numerical Simulation of Bone Adaptation to Mechanical Loading*. PhD Thesis, Stanford University.

Jacobs, C. R., Levenston, M. E., Beaupré, G. S., Simo, J. C., Carter, D. R., 1995. Numerical instabilities in bone remodeling simulations: the advantages of a node-based finite element approach. *Journal of Biomechanics*, vol. 28, pp. 449-459.

Lemaire, V., Tobin, F. L., Greller, L. D., Cho, C. R., Suva, L. J., 2004. Modeling the interactions between osteoblast and osteoclast activities in bone remodeling. *Journal of Theoretical Biology*, v. 229, n. 3, pp. 293 – 309.

Neuert, M. A., Dunning, C. E., 2013. Determination of remodeling parameters for a strain-adaptive finite element model of the distal ulna. Proceedings of the Institution of Mechanical Engineers, Part H: *Journal of Engineering in Medicine*, v. 227, n. 9, pp. 994–1001.

Pérez, M. A., Fornells, P., Doblaré, M., García-Aznar, J. M., 2010. Comparative analysis of bone remodelling models with respect to computerised tomography-based finite element models of bone. *Computer Methods in Biomechanics and Biomedical Engineering*, v. 13, n. 1, pp. 71–80.

Sharma, G. B., Debski, R. E., McMahon, P. J., Robertson, D. D., 2009. Adaptive glenoid bone remodeling simulation. *Journal of Biomechanics*, v. 42, n. 10, pp. 1460 – 1468.

Thomsen, J., Mosekilde, L., Mosekilde, E., 1996. Quantification of remodeling parameter sensitivity—assessed by a computer simulation model. *Bone*, v. 19, n. 5, pp. 505 – 511.

Tsubota, K. ichi, Adachi, T., 2005. Spatial and temporal regulation of cancellous bone structure: Characterization of a rate equation of trabecular surface remodeling. *Medical Engineering & Physics*, v. 27, n. 4, pp. 305 – 311.

Turner, A. W. L. et al., 2005. Computational bone remodelling simulations and comparisons with DEXA results. *Journal of Orthopaedic Research*, Wiley Subscription Services, Inc., A Wiley Company, v. 23, n. 4, pp. 705–712.

Weinans, H., Huiskes, R., Grootenboer, H. J., 1992. The behavior of adaptive bone-remodeling simulation models. *Journal of Biomechanics*, v. 25, pp. 1425–1441.